Journal of Innovative Optical Health Sciences
Vol. 5, No. 4 (2012) 1250022 (7 pages)

DOI: 10.1142/S1793545812500228

AXIAL SUPERRESOLUTION BY PHASE FILTER IN OPTICAL COHERENCE TOMOGRAPHY

ZHIHUA DING*, YANG NI and JIE MENG
State Key Laboratory of Modern Optical Instrumentation
Zhejiang University, Hangzhou 310027, P. R. China
**zh_ding@zju.edu.cn*

Accepted 5 July 2012
Published 9 November 2012

Axial superresolution in optical coherence tomography (OCT) by a three-zone annular phase filter is demonstrated. In the proposed probe of a spectral domain OCT system, the width of the central lobe of the axial intensity point spread function is apodized by the filter to be within the coherence gate determined by the light source, while its sidelobes are lying outside the coherence gate without contributing to the coherence imaging. By measurement of the depth response of the OCT system before and after inserting the filter, an improvement of about 20% in axial resolution is confirmed. OCT imaging on biological sample of orange fresh is also conducted, demonstrating increased depth discrimination without the negative contribution from sidelobes realized by the phase filter in combination with the coherence gate intrinsic to OCT. It comes to a conclusion that we can obtain axial superresolution by filter in OCT system without the degrading influence of large sidelobes.

Keywords: Optical coherence tomography; axial superresolution; phase filter.

1. Introduction

Axial resolution, like transverse resolution, is determined by the numerical aperture (NA) of the focusing lens in a traditional optical system. Higher numerical aperture can achieve better axial resolution. However, a high-NA focusing lens system is more expensive. Furthermore, there is a limitation in improving the NA. There are several methods that can break the diffraction barrier to achieve smaller focal spot, such as apodization,[1] stimulated emission depletion (STED)[2] in fluorescent microscopy, near-field optical microscopy[3] and so on.

The use of a superresolution filter is an effective and convenient approach to reduce the size of a focal spot.[4–6] When a designed pupil filter is applied to a diffraction-limited lens of modest aperture, it causes a narrowness of the central lobe of the intensity point spread function (IPSF). However, this narrowness is accompanied by a big enlargement of sidelobes. If such a combination of lens and pupil filter is used alone, the imaging quality is poor. The large sidelobes spread all over the field producing a background that degrades the image quality, this leads to a serious hindrance in practical application of superresolution in optical imaging systems. Therefore, pupil filters for superresolution are usually applied in confocal system,[7] in which the effective IPSF is a multiplication of both the illuminating PSF and the collecting PSF. Such

multiplication is exploited for reducing sidelobes when two independent pupil filters are designed appropriately.

The reduction of the diffraction-limited spot along the optical axis is known as axial superresolution.[8] There is a very important merit of OCT in implementing superresolution as compared with conventional confocal system and other optical systems. Intrinsic coherence gate of OCT[9] offers the possibility to suppress the axial sidelobes introduced by a superresolving filter. We previously pointed out that sidelobes arising from superresolving filter can be prevented from contributing to the coherence imaging in OCT.[10] By adopting a pupil filter designed with the central lobe of the axial IPSF shrinking to be narrower than the coherence gate and the sidelobes lying outside the coherence gate, it is feasible to obtain an enhanced axial resolution without the negative effect of sidelobes.

As a promising biomedical diagnostic tool, OCT is crying out for high axial resolution. A lot of biomedical applications will benefit from the improvement of axial resolution of OCT. In the case of weakly focused condition, the axial resolution in OCT is mainly determined by the coherence length of the adopted light source. Therefore, previous efforts to enhance axial resolution of OCT focus on developing broadband light sources, such as Kerr-lens mode-locked Ti:sapphire laser,[11] dual beam light sources,[12] spectral shaped light sources,[13] super-continuum generation sources by photonics crystal fiber[14] or tapered fiber,[15] etc. However, such light sources for practical applications are usually costly and complexity in implementation, because limitations exist in finding suitable optical components for broadband transmission. Alternatively, Kulkarni[16] proposed an iterative deconvolution algorithm for enhancing the sharpness of OCT images, which does not recur to the bandwidth of light source. But there is no clear criterion for the image enhancement effect, and this kind of algorithm is mainly suitable in applications of biostructures containing strong, well separated echoes.

In case of tightly focused condition, the width of the central lobe of the axial IPSF is comparative to the width of the coherence gate of OCT. Thus, the axial discrimination ability of OCT is determined by the axial IPSF of the probing objective as well as the bandwidth of the light source. This fact brings out our new method in this paper to improve the axial resolution of OCT by optical superresolution without referring to bandwidth-broadening of light source or deconvolution algorithms for image reconstruction. Considering the power attenuation and the feasibility of fabrication, we propose to adopt a filter based on phase-only pupil function for axial superresolution in OCT. In comparison with conventional amplitude-type filter, a phase-only filter always has better Strehl ratio and can be fabricated with available diffractive optics techniques.

2. Method

Let us consider a general complex pupil function $P(\rho) = T(\rho)\exp[i\varphi(\rho)]$, where ρ is the normalized radial coordinate over the pupil plane, $T(\rho)$ is the transmittance function and $\varphi(\rho)$ is the phase function. The expression of point spread function (PSF) is[17]

$$h(v,u) = 2\int_0^1 P(\rho)J_0(v\rho)\exp(-iu\rho^2/2)\rho d\rho, \quad (1)$$

where v and u are radial and axial dimensionless optical coordinates with origin at the geometrical focus of an optical system, given by $v = kr\cdot\sin\alpha$ and $u = kz\sin^2\alpha$. Here r and z are the usual radial and axial distances, $k = 2\pi/\lambda$, $\sin\alpha$ is the numerical aperture of the objective.

The intensity distribution can be expanded in series near the geometrical focus. The axial and transverse intensity distributions can be expressed to the second order as[18]

$$\begin{aligned} I(0,u) &= |h(0,u)|^2 \\ &= |I_0|^2 - \mathrm{Im}(I_0 I_1^*)u \\ &\quad - \frac{1}{4}[Re(I_0 I_2^*) - |I_1|^2]u^2, \end{aligned} \quad (2)$$

$$I(v,0) = |h(v,0)|^2 = |I_0|^2 - \frac{1}{2}Re(I_0 I_1^*)v^2, \quad (3)$$

where * denotes complex conjugate and I_n is the nth moment of the pupil function, defined as

$$I_n = 2\int_0^1 P(\rho)\rho^{2n+1}d\rho. \quad (4)$$

An annular phase filter consists of a number of zones, each one determined by its radius and phase. We consider binary filters in which the phase are zero and π, thus the pupil moments become

real-valued functions and then the general expressions of Strehl ratio (S), axial gain (G_A) and transverse gain (G_T) are simplified in this form:

$$S = I_0^2, \tag{5}$$

$$G_A = 12\left[\frac{I_2}{I_0} - \left(\frac{I_1}{I_0}\right)^2\right], \tag{6}$$

$$G_T = 2\frac{I_1}{I_0}. \tag{7}$$

We introduce a three-zone binary phase filter whose pupil function is defined as

$$P(\rho) = \begin{cases} \exp(i\varphi_1) = 1 & 0 \le \rho \le a \\ \exp(i\varphi_2) = -1 & a < \rho \le b \\ \exp(i\varphi_3) = 1 & b < \rho \le 1 \end{cases}, \tag{8}$$

where a and b are the normalized inner and outer radius of the middle-zone of the pupil. To keep the transverse resolution unchanged, i.e., $G_T = 1$, an additional constraint $a^2 = 1 - b^2$ is added to let the area of inner-zone and outer-zone to be equal.

Figure 1 shows the axial intensity distribution without filter and with filter corresponding to different a. After considering the axial gain and Strehl ratio, we choose $a = 0.577$, thus we get $b = 0.816$, $G_A = 2.78$, $S = 0.11$.

For a light source with a Gaussian spectrum distribution, its autocorrelation function is given by

$$\gamma(z) = \exp\left[-\left(\frac{\Delta\lambda \cdot \pi \cdot z}{\lambda^2\sqrt{\ln 2}}\right)^2\right], \tag{9}$$

where λ is the center wavelength of the light source, $\Delta\lambda$ is the bandwidth of the light source, and z is the axial depth mismatch, to be half of the path difference. The corresponding width of coherence gate is then determined by

$$\Delta L_C = \frac{2\ln 2}{\pi}\frac{\lambda^2}{\Delta\lambda}. \tag{10}$$

A schematic of an established spectral domain OCT system devoted for axial superresolution by phase filter is illustrated in Fig. 2. The light source is a broadband superluminescent diode with FWHM (Full width at half maximum) bandwidth of 45 nm centered at 835 nm, corresponding to a coherence length of 6.8 μm. Maximum output power of the source is 12 mW. The light is coupled into the

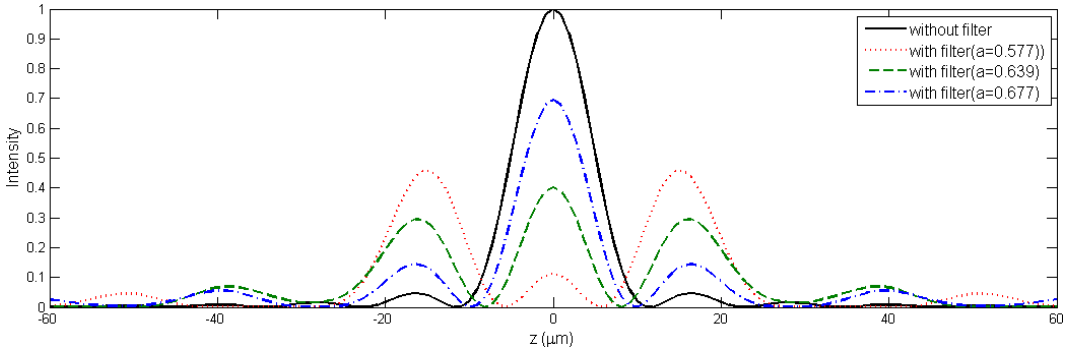

(a)

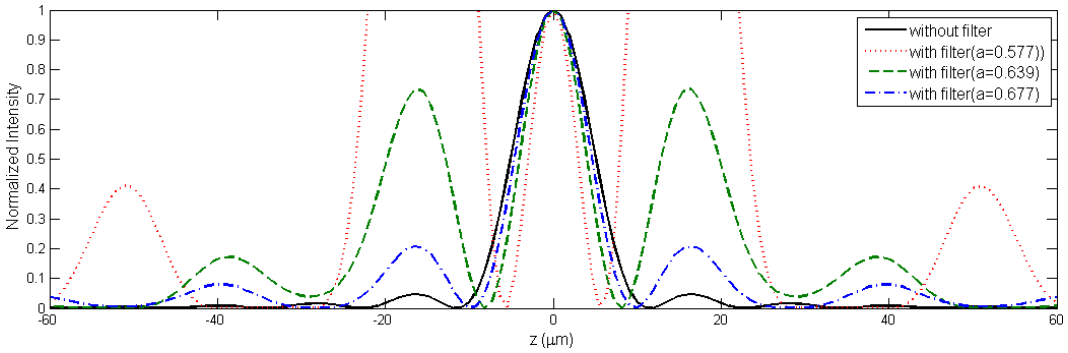

(b)

Fig. 1. Axial intensity distributions near the focus with and without the phase filter (a) and their normalizations (b).

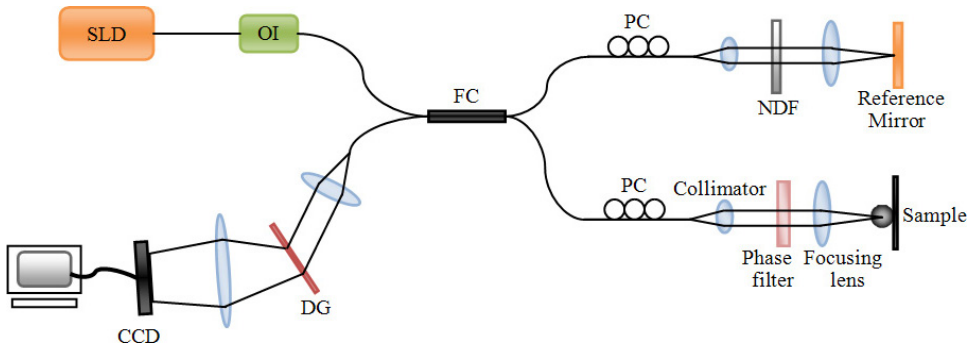

Fig. 2. Spectral domain OCT system for axial superresolution by phase filter, SLD: superluminescent diode, OI: optical isolator, FC: fiber coupler, PC: polarization controller, NDF: neutral density filter, DG: diffraction grating.

fiber-based Michelson interferometer via an optical isolator. The reference light is delivered into a stationary mirror. The sample light passes through the designed phase filter before focused onto the sample by a focusing lens (NA = 0.38). The sample is placed on a two-dimensional translation stage, which is controlled by a step motor for transverse scanning. The reflected and backscattered light from the sample travels back along the same path and interferes with the reference light coming back from the reference arm at the fiber coupler, and the output interference signal is routed into a custom-built spectrometer for detection. The spectrometer consists of a 60 mm focal length achromatic collimating lens, a 1200 lines/mm transmission grating and a 150 mm focal length achromatic lens that images the spectral interference onto a line-scan CCD camera. The camera has 2048 pixels, with each pixel at 14 μm by 14 μm in size and 12-bit in digital depth, with a maximum line scan rate of 29 KHz. The spectral data are transferred to a computer via a high-speed frame grabber board for data processing. The spectrometer has a designed spectral resolution of 0.067 nm, yielding an axial imaging range of 2.56 mm in air on each side of zero delay. The signal sensitivity measured near zero optical path difference is 108 dB with a 16 dB falloff over 2 mm depth range. The polarization controllers are used to optimize the spectral interference fringe contrast at the detector.

Due to confocal characteristics intrinsic to a fiber-based OCT system, the effective axial PSF in the sample arm should be the multiplication of the illuminating axial PSF (h_{in}) and the collecting axial

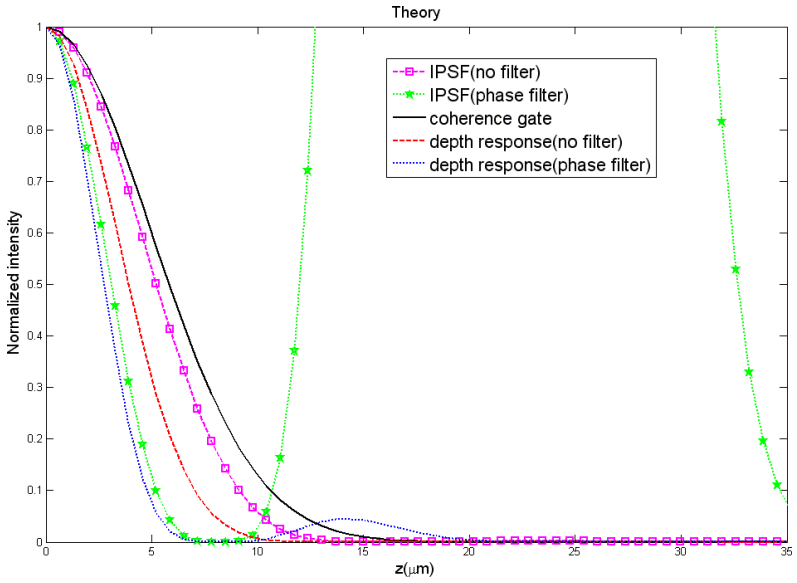

Fig. 3. Theoretical normalized axial IPSF and depth response with and without the phase filter. The solid line represents the signal envelope of the autocorrelation function of the light source, i.e., the coherence gate of OCT.

PSF (h_{out}), i.e., $h_{\text{eff}} = h_{\text{in}} \cdot h_{\text{out}}$. This follows the axial IPSF to be $I_{\text{A}} = |h_{\text{eff}}|^2 = |h_{\text{in}}|^2 \cdot |h_{\text{out}}|^2$. Here, the illuminating axial PSF and the collecting axial PSF are the same.

The depth response function determined by both axial IPSF and coherence gate of OCT is then given by

$$I_{\text{response}} = I_A \cdot \gamma(z). \tag{11}$$

The feasibility of the three-zone phase filter for enhancement of axial resolution in OCT is theoretically analyzed and depicted in Fig. 3. We see that the FWHM of the axial IPSF corresponding to Airy pattern is comparative to the FWHM of the coherence gate of OCT. After inserting the phase filter in the sample arm, a great shrinkage of the central lobe of axial IPSF is achieved. The narrowness of the central lobe introduces undesirable high level sidelobes, which usually degrades image quality in a conventional optical system. However since the first zero of the apodized axial IPSF is falling within the coherence gate intrinsic to the OCT system, these severe sidelobes are suppressed effectively, without any contribution to the coherence imaging. In this case the axial resolution of OCT is determined by the axial focusing geometry of the probing beam as well as the coherence gate, that is, the depth response. Therefore, by adopting the phase filter designed with shrunk central lobe and sidelobes lying outside the coherence gate, it is feasible to realize an enhanced axial resolution while the negative effect of sidelobes is greatly suppressed. The curve of depth response with filter shows the suppression effect of sidelobes by the coherence gate. The FWHM of depth responses with and without filter are calculated to be 2.61 and 3.91 μm, respectively.

3. Experiment

The designed phase-only filter is fabricated and then adopted in the sample arm of the established fiber-based spectral domain OCT system. A reflective mirror with reflectivity higher than 95% is taken as the sample to measure the axial IPSF and depth responses with and without the filter. The measured depth response with and without the three-zone phase filter are shown in Fig. 4. The depth response curves are derived from the demodulation of detected interference signal, which are the combined outcome of the axial IPSF of the objective for probing the sample and the coherence gate intrinsic to the OCT. The experimental curves measured are generally in agreement with the theoretical results. We can see the depth response is shrunk due to the implemented phase filter in the OCT system. The FWHM of depth response with and without filter are respectively 4.09 and 5.21 μm, realizing an improvement of 21% in axial resolution, while the theoretical enhancement is calculated to be 33%. The curves measured are not in perfect accordance with theoretical ones. Such discrepancies between theoretical analyses and the

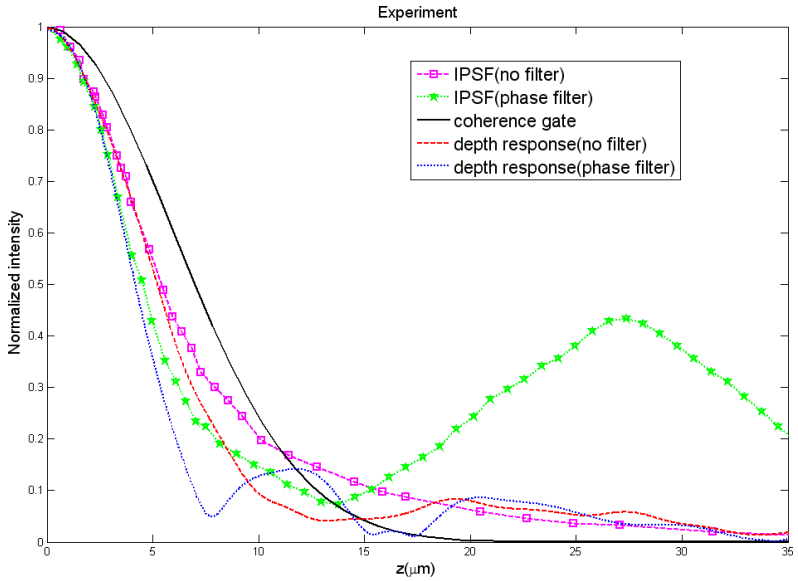

Fig. 4. Measured depth response with and without the phase filter.

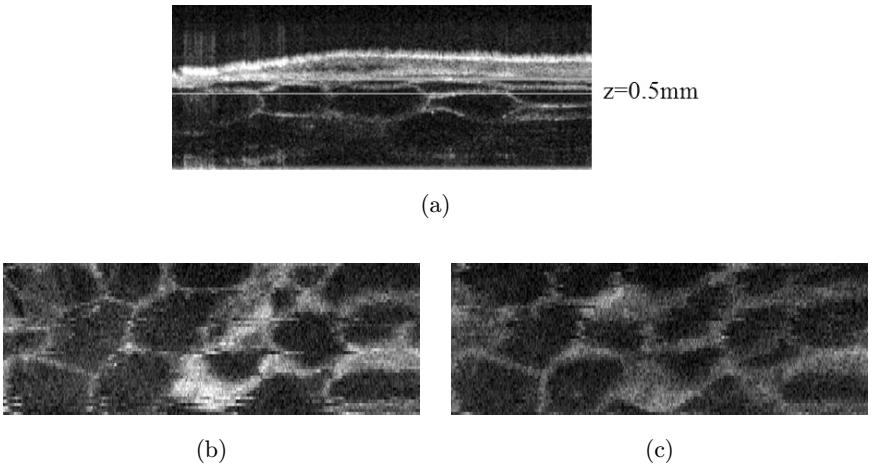

Fig. 5. OCT images of orange fresh, (a) cross-sectional image which indicates the depth of enface image, (b) enface image without filter corresponding to $z = 0.5$ mm, (c) enface image with the phase filter corresponding to $z = 0.5$ mm.

experimental results might be contributed by several factors, including the deviation of the light source spectrum from Gaussian distribution, nonuniformity in illumination upon the filter, inaccurate alignment of the pupil filter, wavelength dependent phase errors in filter design and dispersion mismatch between interference beams in OCT system.

To study the feasibility of achieving axial superresolution by the proposed method for biological sample, OCT imaging of orange fresh are conducted. As demonstrated in Fig. 5, cross-sectional image of the orange fresh is shown in Fig. 5(a), where a horizontal line indicates the focusing depth corresponding to $z = 0.5$ mm of the objective. Enface images corresponding to focusing position around $z = 0.5$ mm achieved without and with the phase filter are shown in Figs. 5(b) and 5(c), respectively. We see that some horizontal lines evident in Fig. 5(b) are disappeared in Fig. 5(c), due to the increased depth discrimination realized by the phase filter adopted in the OCT system. Furthermore, artifacts due to sidelobes introduced by the phase filter are no observed in Fig. 5(c), demonstrating that the coherent gate intrinsic to OCT could be useful in suppressing the negative contribution of the apodization phase filter. We also notice that light power attenuation induced by the phase filter is evident in Fig. 5(c) in comparison with Fig. 5(b). The loss of power due to the phase filter is estimated to be around 9.5 dB. However, such attenuation is not a serious problem since OCT adopts heterodyne detection and logarithmic mapping of detected signal. One thing should be mentioned is the negative effect of the sidelobes caused by phase filter on lateral resolution.

4. Conclusion

By adopting a three-zone phase filter in front of the focusing lens of the sample arm, we demonstrate theoretical and experimental evidence for an effective increase of about 20% in axial resolution of OCT under tightly focusing condition. In the proposed probe of the spectral domain OCT system, the width of the central lobe of the axial IPSF is narrowed within the coherence length of the light source, while its sidelobes are lying outside without contributing to coherence imaging. The designed phase-only filter has realized the purpose of axial resolution enhancement, but discrepancy exists between theoretical and experimental results due to several factors. Further works are required to eliminate these influences and designing other pupil filter appropriated for axial superresolution. The proposed method to enhance the axial resolution of OCT by combining coherence gate with optical superresolution is economical and convenient in instrumentation.

Acknowledgment

This work was supported by the National Natural Sciences Foundation of China (60978037, 60878057).

References

1. R. Heintzmann, T. M. Jovin, C. Cremer, "Saturated patterned excitation microscopy — a concept for optical resolution improvement," *J. Opt. Soc. Am. A* **19**(8), 1599−1609 (2002).
2. M. A. Schwentker, H. Bock, M. Hofmann, S. Jakobs, J. Bewersdorf, C. Eggeling, S. W. Hell, "Wide-field subdiffraction RESOLFT microscopy using fluorescent protein photoswitching," *Microsc. Res. Tech.* **70**(3), 269−280 (2007).
3. E. Betzig, J. K. Trautman, T. D. Harris, J. S. Weiner, R. L. Kostelak, "Breaking the diffraction barrier: Optical microscopy on a nanometric scale," *Science* **251**(5000), 1468−1470 (1991).
4. T. R. M. Sales, G. M. Morris, "Diffractive superresolution elements," *J. Opt. Soc. Am. A* **14**(7), 1637−1646 (1997).
5. T. R. M. Sales, G. M. Morris, "Fundamental limits of optical superresolution," *Opt. Lett.* **22**(9), 582−584 (1997).
6. H. Luo, C. Zhou, "Comparison of superresolution effects with annular phase and amplitude filters," *Appl. Opt.* **43**(34), 6242−6247 (2004).
7. Z. Ding, G. Wang, M. Gu *et al.*, "Superresolution using an apodization film in a confocal setup," *Appl. Opt.* **36**(1), 360−363 (1997).
8. T. R. M. Sales, G. M. Morris, "Axial superresolution with phase-only pupil filters," *Opt. Commun.* **156**(4−6), 227−230 (1998).
9. A. F. Fercher, W. Drexler, C. K. Hitzenberger, T. Lasser, "Optical coherence tomography — principles and applications," *Rep. Prog. Phys.* **66**(2), 239−303 (2003).
10. L. Zhou, Z. Ding, X. Yu, "Depth superresolution in optical coherence tomography through the combination of apodization and coherence gating," *Acta Opt. Sin.* **25**(9), 1181−1185 (2005).
11. U. Morgner, F. X. Kärtner, S. H. Cho, Y. Chen, H. A. Haus, J. G. Fujimoto, E. P. Ippen, V. Scheuer, G. Angelow, T. Tschudi, "Sub-two cycle pulses from a Kerr-lens mode-locked Ti:sapphire laser," *Opt. Lett.* **24**(6), 411−413 (1999).
12. A. Baumgartner, C. K. Hitzenberger, H. Sattmann, W. Drexler, A. F. Fercher, "Signal and resolution enhancements in dual beam optical coherence tomography of the human eye," *J. Biomed. Opt.* **3**(1), 45−54 (1998).
13. S. Sun, J. Guo, J. Gao, P. Xue, "Enhancement of optical coherence tomography axial resolution by spectral shaping," *Chin. Phys. Lett.* **19**(10), 1456−1458 (2002).
14. Y. Wang, Y. Zhao, J. S. Nelson, Z. Chen, R. S. Windeler, "Ultrahigh-resolution optical coherence tomography by broadband continuum generation from a photonic crystal fiber," *Opt. Lett.* **28**(3), 182−184 (2003).
15. T. A. Birks, W. J. Wadsworth, P. S. J. Russell, "Supercontinuum generation in tapered fibers," *Opt. Lett.* **25**(19), 1415−1417 (2000).
16. M. D. Kulkarni, C. W. Thomas, J. A. Izatt, "Image enhancement in optical coherence tomography," *Electron. Lett.* **33**(16), 1365−1367 (1997).
17. M. Born, E. Wolf, *Principle of Optics*, Chap. 8 (Oxford, Pergamon Press, 1975).
18. D. M. de Juana, J. E. Oti, V. F. Canales, M. P. Cagigal, "Design of superresolving continuous phase filters," *Opt. Lett.* **28**(8), 607−609 (2003).